Velocity statistics for interacting edge dislocations in one dimension from Dyson's Coulomb gas model

Farshid Jafarpour,[1] Luiza Angheluta,[1,2] and Nigel Goldenfeld[1]

[1]*Department of Physics, University of Illinois at Urbana-Champaign, Loomis Laboratory of Physics, 1110 West Green Street, Urbana, Illinois 61801-3080, USA*

[2]*Physics of Geological Processes, Department of Physics, University of Oslo, Norway*

(Received 20 June 2013; published 14 October 2013)

The dynamics of edge dislocations with parallel Burgers vectors, moving in the same slip plane, is mapped onto Dyson's model of a two-dimensional Coulomb gas confined in one dimension. We show that the tail distribution of the velocity of dislocations is power law in form, as a consequence of the pair interaction of nearest neighbors in one dimension. In two dimensions, we show the presence of a pairing phase transition in a system of interacting dislocations with parallel Burgers vectors. The scaling exponent of the velocity distribution at effective temperatures well below this pairing transition temperature can be derived from the nearest-neighbor interaction, while near the transition temperature, the distribution deviates from the form predicted by the nearest-neighbor interaction, suggesting the presence of collective effects.

DOI: 10.1103/PhysRevE.88.042123 PACS number(s): 64.60.av, 05.10.Gg, 61.72.Ff

I. INTRODUCTION

At mesoscopic scales, crystalline materials under stress exhibit intermittent behavior through plastic slip avalanches that follow the power-law statistics predicted by the mean field theory of interface depinning transition [1–10]. The origin of intermittency in plastic strain rate fluctuations is attributed to the collective dynamics of dissipative structures, such as dislocations, where shear deformation is localized. In addition to the heterogeneous strain response, the long range elastic interactions between dislocations lead to complex spatial-temporal patterning and correlations [11]. Plastic slip avalanches mediated by dislocations have been studied numerically using discrete dislocation dynamics models [2,12,13] and phase field crystal models [10].

A point edge dislocation generates in two dimensions a shear stress that decays as $1/|\vec{r}|$ with a quadrupole anisotropy of the form

$$\tau(\vec{r}) = b\mu \frac{x(x^2 - y^2)}{2\pi(1-\nu)(x^2+y^2)^2}, \tag{1}$$

where $\vec{r} = (x, y)$ is a position vector with respect to the dislocation origin, b is the length of the Burgers vector parallel to the x direction ($\vec{b} = b\hat{x}$), μ is the shear modulus, and ν is the Poisson ratio [14]. The discrete dislocation dynamics (DDD) model describes a collection of N edge dislocations with pairwise interactions mediated by the internal shear stress τ from Eq. (1). Each dislocation performs an overdamped motion along the x direction described by [2,12,15]

$$\frac{\eta}{b}\frac{dx_i}{dt} = b\sum_{j\neq i}\tau(\vec{r}_i - \vec{r}_j), \qquad \forall i = 1, \ldots, N, \tag{2}$$

where η/b is an effective friction coefficient per unit dislocation length [16]. Most of the DDD simulations are done at zero temperature and focus on the collective effects of dislocations in the presence of an external, uniform stress. Starting from a random configuration, the system relaxes according to Eq. (3) towards a frozen metastable configuration. At a nonvanishing external stress below a critical threshold, the relaxation dynamics follows a power-law scaling in time with exponents depending on the physical setup [16,17]. Above a critical threshold and after a transient power-law relaxation, the system approaches a stress-dependent plateau corresponding to steady-state plastic flow.

Since the velocity of each dislocation is proportional to the stress at the position of the dislocation, in a translationally invariant system, where the probability density of position of dislocations is uniform, the distribution of velocity v of dislocations has the same functional form as the distribution of internal stress. Although the velocity distribution of individual dislocations (or, equivalently, the distribution of internal stress) has not been directly measured, from a theoretical point of view, it is a better defined quantity compared to the distribution of acoustic energy of plastic slip avalanches, as one does not need to deal with the arbitrarily defined thresholds and coarse-graining time scales that show up in the definition of slip events in avalanches. Also, in a discrete dislocation dynamics simulation, as a measure of the statistical properties of the system, the stress distribution can be numerically calculated and analyzed more effectively than the pair correlation function [18].

While the local stress fluctuations are known to be power-law distributed, different exponents have been found in the literature depending on the details of the models and methods used in the particular studies. The probability distribution of stress is analytically studied in Ref. [19] for a two-dimensional statistical model, and a power-law scaling τ^{-3} is found for the high stress tail of the stress distribution in equilibrium configurations. A similar power law, found in the high velocity tail of the velocity distribution in both two and three dimensions in discrete dislocation dynamics simulation in Ref. [20], is attributed to the avalanche dynamics and has been shown to be independent of the value of the external stress. However, at intermediate stresses, when a pair of oppositely oriented dislocations can be approximated by ideal dipoles, the stress distribution has been shown to have the exponent -2 [18]. Reference [2] shows that the $E^{-3/2}$ distribution of the acoustic energy, E, of avalanches that is measured

experimentally is associated with the power-law distribution of velocity of dislocations with an exponent -2.5 that is again independent of the value of the external stress. In this study, the presence of avalanches and intermittency of the system was attributed to dislocation pair-creation through Frank-Read sources.

In Refs. [2,5,20,21] discussed above, the robust power-law distributions for the different avalanche variables of the collective dislocation dynamics are attributed to self-organized criticality, while other studies [8,10,22,23] show that, in fact, the avalanche statistics is a signature of a fine-tuned critical behavior predicted by the mean field depinning transition. Reference [22] derives the density dependence of the critical stress below which the system of dislocations are jammed and proposes a phase diagram by analogy with the jamming transition in granular materials [24] in which stress and temperature play symmetric roles.

Although the DDD method has been extensively used to investigate plastic flow problems, most studies are based on a deterministic, athermal approach. Hence, the classical DDD model is not suitable for simulating thermally activated processes, such as dislocation-obstacle interactions. In athermal DDD simulations, the system gets trapped into a metastable configuration, causing unphysical freezing of dislocation motion. Hence, it is challenging to study equilibrium properties of dislocation ensembles in athermal configurations. Instead, we consider a stochastic approach by including in the dislocation motion, given by Eq. (3), random stress pulses that mimic, to a first approximation, thermal agitations. Another source of stochasticity in dislocation dynamics is the fluctuating local strain field arising from random dislocation arrangements. This approach has been applied to study the distribution of stress fluctuations [19] and fractal dislocation patterning during plastic deformations [25,26].

The purpose of this paper is to investigate the statistical properties of equilibrium dislocation configurations in the presence of thermal fluctuations. Thermal agitations arise from random collisions of dislocations with surrounding particles, such as phonons, and result in random forces acting on dislocations. The stochastic version of Eq. (2) that we consider is given by

$$\frac{\eta}{b}\frac{dx_i}{dt} = b\sum_{j\neq i}\tau(\vec{r}_i-\vec{r}_j)+\xi_i(t), \tag{3}$$

where the fluctuations are Gaussian distributed with zero mean and variance,

$$\langle \xi_i(t)\xi_j(t')\rangle = \frac{2k_BT\eta}{b^2}\delta_{i,j}\delta(t-t'), \tag{4}$$

which depends on the effective temperature k_BT and a damping coefficient consistent with the fluctuation-dissipation theorem. In particular, we study the distribution of velocities of dislocations in a relaxed configuration and show that the corresponding power-law probability distribution function $P(v)$ is not necessarily a collective effect arising from avalanches dynamics, nonequilibrium critical points, or self-organized criticality; rather, it is a consequence of the functional form of the stress in Eq. (1) and, in some cases, can be determined only by considering the nearest-neighbor interaction. In other cases, where the collective dynamics of dislocations has a significant effect on $P(v)$, this collective effect can be quantified by considering the deviation of the exponent of the power-law distribution of velocity from the one predicted using only the nearest-neighbor interaction. In Sec. II, we show that Eq. (3) in one dimension is the same as the equation of motion for a two-dimensional (2D) Coulomb gas confined in one dimension (1D). This system is sometimes known as Dyson's model and was first introduced to investigate the statistical properties of energy levels of heavy nuclei [27]. We find the probability distribution of velocity in Dyson's model and show that it follows a temperature-dependent power-law distribution which can be predicted simply by considering the nearest-neighbor interaction and thus is a consequence of the logarithmic interaction energy.

The nearest-neighbor analysis in 2D is performed in Sec. III, where we find a power-law distribution of velocities with an exponent -2 independent of the effective temperature. We show the presence of a phase transition analogous to the pairing transition in a 1D plasma with logarithmic interaction [28] at a temperature where the effective thermal energy becomes equal to the mutual interaction energy scale $\frac{\mu b^3}{2\pi(1-\nu)}$. Above this temperature, the dislocations are no longer bound to their nearest neighbor in the long time limit. At temperatures well below the transition temperature, we show that the nearest-neighbor approximation is valid, and the probability distribution of velocities of dislocations follows a power-law with the exponent -2, while at temperatures comparable with the transition temperature or above, the exponent of the power-law distribution of velocity deviates from -2 and is thus a presumptive indication of the collective dynamics of dislocations.

II. VELOCITY DISTRIBUTION IN DYSON'S MODEL

In 1D, Eq. (1) for the internal stress simplifies to a $1/r$ force, such that Eq. (3) reduces to the stochastic equation of motion for a 2D Coulomb gas confined in 1D, which was first studied by Dyson [27] to investigate the statistics of the energy levels of heavy nuclei. Dyson's model has also been used to model a wide variety of phenomena in nuclear physics and other fields, including random matrix theory [29,30], the theory of orthogonal polynomials [31,32], and quantum transport theory [29,33]. Since a system of Coulomb particles with the same charge (in our case, dislocations with the same Burgers vector) does not have a stable equilibrium, a uniform background of opposite charge is added to the model through a parabolic potential term, keeping the particles from flying off to infinity.

Here we work with a dimensionless spatial variable $\hat{x}$ by rescaling the length in units of the Burgers vector, $x = b\hat{x}$, and define a dimensionless time variable $\hat{t}$ through $t \equiv \hat{t}t_0$, with $t_0 = 2\pi(1-\nu)\eta/(b\mu)$. In these units and dropping the hat symbol over the dimensionless variables, Eq. (3) with an additional term $-\kappa x_i$, added to ensure the charge neutrality condition, can be written as

$$\frac{dx_i}{dt} = \sum_{j\neq i}\frac{1}{x_i-x_j} - \kappa x_i + \xi_i(t), \tag{5}$$

which is the same as the equation of motion in Dyson's model [27]. The value of the dimensionless parameter κ

is an indication of the strength of the parabolic potential originating from the uniform opposite charge background, and it introduces a new length scale in the problem. We show that the addition of the parabolic potential does not influence the power-law distribution of the velocity of dislocations and its only function is to keep the system bounded. The variance of the dimensionless fluctuations is then given by

$$\langle \xi_i(t)\xi_j(t')\rangle = 2\sigma\delta_{ij}\delta(t-t'), \tag{6}$$

where $\sigma = 2\pi(1-\nu)k_BT/(\mu b^3)$, which is the ratio between the effective thermal energy and the elastic interaction energy. From Eq. (5), the Fokker-Plank equation for the joint probability distribution of the positions of dislocations $\rho(x_1,\ldots,x_N,t)$ follows as

$$\frac{\partial\rho}{\partial t} = \sigma\sum_i \frac{\partial^2\rho}{\partial x_i^2} - \sum_i \frac{\partial}{\partial x_i}\left[\rho\left(\sum_{j\neq i}\frac{1}{x_i-x_j} - kx_i\right)\right]. \tag{7}$$

The equilibrium configurational probability distribution is determined from Eq. (7) and is given by [27]

$$\rho(x_1,\ldots,x_N) \propto \left(\prod_{i<j}|x_i-x_j|^{1/\sigma}\right)\exp\left(-\frac{\kappa}{2\sigma}\sum_i x_i^2\right). \tag{8}$$

However, the exact probability distribution of particle velocities in this system is very difficult to determine, due to the nonlinear relationship between the x_i's and the v_i's in Eq. (5). Nonetheless, we show that the velocity distribution can be computed analytically in the limit where only the nearest-neighbor interactions are dominant. This is done by solving the system of two particles and comparing with the numerical result for a simulated system of $N = 100$ particles. The strength of the parabolic potential for the two-body system is tuned to give the same average separation between the particles as the one in the simulation.

Let the vector $\vec{x} \equiv (x_1,x_2)$ be the position vector of two particles and $\vec{v} \equiv (v_1,v_2)$ be the deterministic part of the velocity vector:

$$\vec{v}(\vec{x}) = \left(\frac{1}{x_1-x_2} - \kappa x_1, \frac{1}{x_2-x_1} - \kappa x_2\right). \tag{9}$$

The joint probability distribution of velocities can be found by the change of variables $\vec{x} \to \vec{v}$ in the probability distribution of positions,

$$P(\vec{v}) = \sum_{\vec{x}(\vec{v})}\rho[\vec{x}(\vec{v})]\left|\begin{array}{cc}\frac{\partial x_1}{\partial v_1} & \frac{\partial x_1}{\partial v_2}\\ \frac{\partial x_2}{\partial v_1} & \frac{\partial x_2}{\partial v_2}\end{array}\right|, \tag{10}$$

where the summation is performed over all the positions $\vec{x}$ associated with the same velocity $\vec{v}$ in Eq. (9). By inverting Eq. (9) and substituting in Eq. (8), the joint probability distribution of velocities $P(\vec{v})$ can be written as

$$P(\vec{v}) = C\exp\left(\frac{w^2}{\kappa\sigma}\right)\sum_{+,-}\frac{1}{\sqrt{u^2+8\kappa}}(\mp u+\sqrt{u^2+8\kappa})^{1+\frac{1}{\sigma}} \times \exp\left(-\frac{u^2\mp u\sqrt{u^2+8\kappa}}{8\kappa\sigma}\right), \tag{11}$$

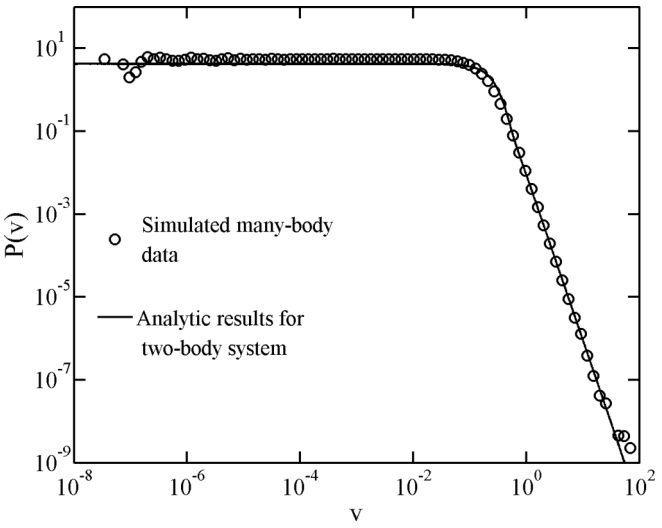

FIG. 1. Probability distribution of velocity of particles at $\sigma = 1/2$. The solid line is the result of numerical integration of (11) with $\kappa = 0.05$. The circles are the data from the simulation of a system of $N = 100$ particles with $\kappa = 10^{-3}$.

where $u = v_1 - v_2$ and $w = \frac{1}{2}(v_1+v_2)$ are the relative and center-of-mass velocities, respectively, and C is a normalization constant. Equation (11) can be numerically integrated over either v_1 or v_2 to obtain the probability distribution of velocity. In Fig. 1, we compare the result of numerical integration of Eq. (11) with the simulation of a system of $N = 100$ particles at $\sigma = \frac{1}{2}$. In order to obtain the same transition velocity (the velocity at which $P(v)$ becomes a power law), κ was scaled up by a factor of 50 to keep κN constant.

In the high velocity limit (either $v_1 \to \infty$ or $v_2 \to \infty$), Eq. (11) scales as

$$P(\vec{v}) \sim |u|^{-2-1/\sigma}. \tag{12}$$

We claim that almost all of the high velocity events result from the pair interaction of two particles that are very close to each other. Therefore, in this limit, v_1 and v_2 would be correlated ($v_1 \sim -v_2$), implying that $P(v)$ also scales as

$$P(v) \sim |v|^{-2-1/\sigma}, \tag{13}$$

where $v = |v_1| = |v_2|$. Figure 2 shows how the tail of the probability distribution of velocities scales for different values of σ. The exponent $\beta = -2 - 1/\sigma$ is independent of κ as expected. In fact, the same result can be obtained without the parabolic potential, by calculating the probability distribution for the velocity of a movable particle trapped in between two fixed particles. In this case, to get the correct transition velocity, the separation of two fixed particles should be set to twice the most likely next-neighbor separation of particles obtained from a many-body simulation. This is a clear indication that the only effect of the background parabolic potential is to keep the system bounded and that it does not affect the scaling of the velocity distribution.

Given the functional form of the pair interaction ($1/r$ force) and the claim that high velocity events are consequences of very close neighbor interactions, we can understand the power-law tail of the velocity distribution through the following scaling argument: Since $r \to 0$ is a singular limit, for two

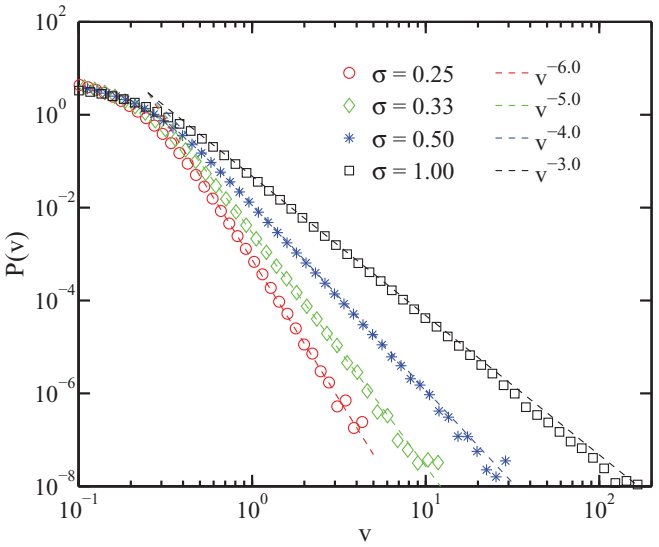

FIG. 2. (Color online) High velocity tail of probability distribution of velocities for $\sigma \in \{\frac{1}{4}, \frac{1}{3}, \frac{1}{2}, 1\}$ for $N = 100$ particles with $\kappa = 10^{-3}$. The exponent of the power-law distribution agrees with predicted values from Eq. (13).

very close particles, both the external force (the force from the parabolic potential in this case) and the superposition of all forces from other distant particles can be neglected compared to the force of the closest particle. Therefore, $v(r)$ scales as $v \sim 1/r$. Also, from Eq. (8), $\rho(r)$ scales as $\rho(r) \sim r^{1/\sigma}$. Using

$$\rho(r)dr = P(v)dv, \tag{14}$$

we have

$$P(v) \sim \rho[r(v)]\left|\frac{dr}{dv}\right| \sim v^{-2-1/\sigma}. \tag{15}$$

It is important to confirm that $\rho(r) \sim r^{1/\sigma}$; that is, we can neglect the contribution of the interactions with other particles in the scaling of the probability distribution separation of

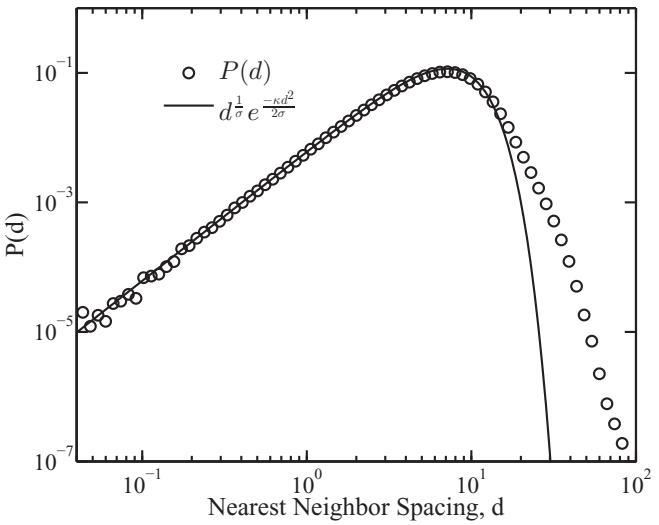

FIG. 3. Probability distribution $P_{\rm nn}$ of the nearest-neighbor separation, d, for a system of $N = 100$ particles compared with the distribution of relative distance in a two-body system.

a pair of particles with very small distance. Equivalently, we need to confirm that the distribution of nearest-neighbor separation is the same as the two-particle distribution in the limit of small distance. Figure 3 compares the probability distribution $P_{\rm nn}(d)$ of the nearest-neighbor separation, d, with the distribution of relative distance in a two-body system. Although the distribution at large separations behaves differently in the many-body system from the two-body system, the small separation limits of both systems are essentially identical.

From the simple argument above, it is clear that the temperature-dependent power-law distribution of velocities in 1D is not a collective effect, and it is only a consequence of the logarithmic interaction potential. The distribution of velocities and the short distance limit of the distribution of nearest-neighbor separations can be very well approximated with those of the two-body system. The long distance limit of the distribution of the nearest-neighbor separations is the only quantity that cannot be predicted from the two-body analysis (see Fig. 3).

III. TWO-DIMENSIONAL MODEL AND PAIRING TRANSITION

A neutral system of dislocations with opposite charges in 1D is difficult to study without introducing ad-hoc rules of pair creation and annihilation. Forrester has studied a 2D generalization of Eq. (5) for a system with two opposite charges and isotropic logarithmic interaction potential [34]. For nanocrystals with strong crystal anisotropy, the assumption of straight edge dislocations with parallel Burgers vectors is a good approximation, and, in this case, the motion is confined to discrete, parallel glide lines. However, the dislocation interaction is not a simple isotropic logarithmic potential, but it obeys Eq. (1). We can generalize Dyson's model with an anisotropic interaction as following.

Consider a system of $2N$ particles (N of each charge) with position vectors $\vec{r}_i^{\pm} = (x_i^{\pm}, y_i^{\pm})$ $(1 \leqslant i \leqslant N)$, where $y_i^{\pm}$'s are a set of $2N$ uniformly distributed random variables between 0 and L, and $x_i^{\pm}$'s satisfy the following equations of motion:

$$\frac{dx_i^{\pm}}{dt} = \sum_{j\neq i} \tau(\vec{r}_i^{\pm} - \vec{r}_j^{\pm}) - \sum_j \tau(\vec{r}_i^{\pm} - \vec{r}_j^{\mp}) + \sqrt{2\sigma}\xi_i^{\pm}(t). \tag{16}$$

Here

$$\tau(\vec{r}) = \frac{x(x^2 - y^2)}{(x^2 + y^2)^2}, \tag{17}$$

and $\langle \xi_i^{\pm}(t)\xi_j^{\pm}(t')\rangle = \delta_{ij}\delta(t - t')$.

Since the system is charge neutral, the term from the parabolic potential is no longer necessary. We notice that Eq. (17) can be derived from a potential of the form

$$V(\vec{r}) = -\frac{y^2}{|\vec{r}|^2} - \log(|\vec{r}|). \tag{18}$$

The equilibrium joint probability distribution for the positions of these particles is given by the generalization of Eq. (8) to a

neutral system of particles and has the following expression:

$$\rho(\vec{r}_1^+,\ldots,\vec{r}_N^+,\vec{r}_1^-,\ldots,\vec{r}_N^-)=\frac{1}{\mathcal{Z}}\frac{\prod_{i<j}|\vec{r}_i^+-\vec{r}_j^+|^{\frac{1}{\sigma}}\exp\left(\frac{(y_i^+-y_j^+)^2}{\sigma|\vec{r}_i^+-\vec{r}_j^+|^2}\right)\prod_{n<m}|\vec{r}_n^--\vec{r}_m^-|^{\frac{1}{\sigma}}\exp\left(\frac{(y_n^--y_m^-)^2}{\sigma|\vec{r}_n^--\vec{r}_m^-|^2}\right)}{\prod_{i,j}|\vec{r}_i^+-\vec{r}_j^-|^{\frac{1}{\sigma}}\exp\left(\frac{(y_i^+-y_j^-)^2}{\sigma|\vec{r}_i^+-\vec{r}_j^-|^2}\right)}, \tag{19}$$

where the partition function is expressed as

$$\mathcal{Z}=L^{2N}\int d^{2N}r\frac{\prod_{i<j}|\vec{r}_i^+-\vec{r}_j^+|^{\frac{1}{\sigma}}\exp\left(\frac{(y_i^+-y_j^+)^2}{\sigma|\vec{r}_i^+-\vec{r}_j^+|^2}\right)\prod_{n<m}|\vec{r}_n^--\vec{r}_m^-|^{\frac{1}{\sigma}}\exp\left(\frac{(y_n^--y_m^-)^2}{\sigma|\vec{r}_n^--\vec{r}_m^-|^2}\right)}{\prod_{i,j}|\vec{r}_i^+-\vec{r}_j^-|^{\frac{1}{\sigma}}\exp\left(\frac{(y_i^+-y_j^-)^2}{\sigma|\vec{r}_i^+-\vec{r}_j^-|^2}\right)}. \tag{20}$$

We show that the logarithmic term in Eq. (18) results in a power-law velocity distribution for a system of two particles. If the power-law distribution of velocities is a consequence of the nearest-neighbor pair interaction, as was the case in a 1D system with one charge, we should be able to predict the exponent of the velocity distribution in a many-body system by studying a system of two particles. However, if the high velocity events are dominated by collective effects such as avalanches, we should see different exponents in the many-body simulation compared to the analysis of the two-body system. We show that, in fact, the latter is true, and at a nonzero temperature, the high velocity events are dominated by collective interactions.

In contrast to the case of same-charge particles in 1D, the opposite charges have attractive forces, and therefore, the nearest neighbor of each particle is expected to have the opposite charge for the majority of the time when the system is at equilibrium. Consider a system of two opposite charges moving on two parallel lines with separation $y=y^+-y^-$ and relative longitudinal displacement $x=x^+-x^-$ obeying the equation of motion

$$\frac{dx}{dt}=-2\frac{x(x^2-y^2)}{(x^2+y^2)^2}+\sqrt{4\sigma}\xi(t). \tag{21}$$

This equation imposes a limit of $v_{\max}=\frac{1}{4y}$ on the absolute value of the velocity of these particles. The absolute value of velocity attains its maxima at $x=\pm(1\pm\sqrt{2})y$.

Equation (21) is simplified through rescaling x by y. This corresponds to the changes of variables $\frac{x}{y}\to x$, $\frac{t}{y^2}\to t$, and $y\xi\to\xi$. Under these changes of variables, Eq. (21) becomes

$$\frac{dx}{dt}=-2\frac{x(x^2-1)}{(x^2+1)^2}+\sqrt{4\sigma}\xi(t), \tag{22}$$

which is the same equation obtained by setting $y=1$. From Eqs. (19) and (20), we have

$$\rho(x)=\frac{1}{\mathcal{Z}}(x^2+1)^{-\frac{1}{2\sigma}}\exp\left(-\frac{1}{\sigma(x^2+1)}\right) \tag{23}$$

and

$$\mathcal{Z}=\int_{-\infty}^{+\infty}(x^2+1)^{-\frac{1}{2\sigma}}\exp\left(-\frac{1}{\sigma(x^2+1)}\right)dx. \tag{24}$$

The integral above converges only for $\sigma<1$, meaning that for $\sigma\geqslant 1$, at equilibrium, the probability of finding the particles at any finite separation is zero. At low temperatures, the particles remain in a bound state at equilibrium. Above the critical temperature $\sigma_c=1$, the particles are no longer bound and fly off to infinity in the long time limit. This is the analog of the pairing transition in a 1D plasma with logarithmic interaction with a short distance cutoff [28].

The probability distribution for the relative velocity of these particles can be found using the change of variable

$$P(v)=\sum_{x(v)}\rho[x(v)]\left|\frac{dx}{dv}\right|. \tag{25}$$

Figure 4 shows the resulting velocity distribution calculated from Eq. (25) for temperatures $\sigma=\frac{2}{3}$ and $\frac{3}{4}$. The divergence of $P(v)$ at $v_{\max}$ is due to the singular change of variable Jacobian $|\frac{dx}{dv}|$. For $\sigma>\frac{1}{2}$, away from the maximum velocity, corresponding to $|x|\gg 1$, $P(v)$ decays as

$$P(v)\sim v^{-2+1/\sigma}. \tag{26}$$

In this region, the system can be approximated by the 1D system, and an argument similar to the one in the previous section can be used to explain the scaling behavior of $P(v)$. For $\sigma\leqslant 1/2$, however, the $x\gg 1$ region has a finite contribution in the low velocity limit [$\lim_{v\to 0}P(v)$ is finite for $\sigma\leqslant 1/2$ in Eq. (26)], and therefore, the contributions of other zeros of velocity near $x=0$ become important. In this region, the low velocity scaling of $P(v)$ can be determined by considering the contributions of all the competing terms from zeros of velocity including both the ones near zero and the one at infinity in the scaling argument.

$P(v)$ calculated above is, in fact, the conditional probability distribution for the velocity given the separation $y=1$ or $P(v|y=1)$. The relation

$$P(v|y)=yF(yv) \tag{27}$$

can be obtained by a reverse change of variable to the original x, y, and v, where $F(v)=P(v|y=1)$ is the distribution calculated above. In order to calculate the probability distribution for the velocity, independent of y,

$$P(v)=\int_0^\infty P(v|y)f(y)dy, \tag{28}$$

the distribution of y, $f(y)$, is needed. In the original many-body problem, y_i's were chosen to be uniformly distributed. However, the two-body problem that approximates the many-body problem is constructed to represent a pair of nearest neighbors in the many-body problem. Thus, $f_N(y)$ should be

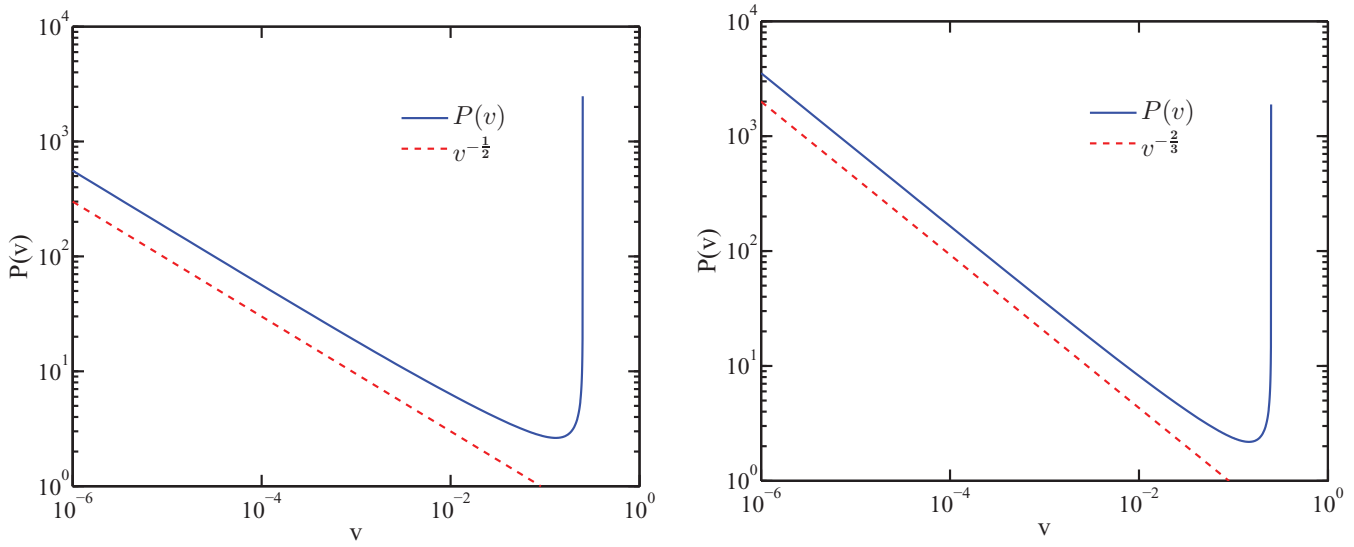

(a) $\sigma = \frac{2}{3}$ (b) $\sigma = \frac{3}{4}$

FIG. 4. (Color online) Relative velocity distribution calculated from Eq. (25) for temperatures $\sigma \in \{\frac{2}{3}, \frac{3}{4}\}$ compared with the predicted power law in Eq. (26).

defined to be the probability distribution of the distance from the nearest neighbor in an ensemble of N uniformly distributed y_i's, $0 \leqslant y_i \leqslant L = Nd$, for some average separation d. In other words, $f_N(y)$ is the probability of finding y_i at any point $0 \leqslant s \leqslant L = dN$, finding another y_j at the distance y from y_i, and finding all the other y_k's outside of the interval $(s - y, s + y)$, given that the probability density of finding each y_i at each point in $(0, L)$ is $L^{-1} = (Nd)^{-1}$:

$$\begin{aligned} f_N(y) &= \int_0^{Nd} P(y_i = s) \sum_{j \neq i} \Bigg[P(y_j = s \pm y) \\ &\quad \times \prod_{k \neq i,j} \left(1 - \int_{\max\{s-y,0\}}^{\min\{s+y,Nd\}} P(y_k = x) dx \right) \Bigg] ds \\ &\approx Nd \left(\frac{1}{Nd} \right) (N-1) \left[\frac{2}{Nd} \left(1 - \frac{2y}{Nd} \right)^{N-2} \right] \\ &= \frac{2(N-1)}{Nd} \left(1 - \frac{2y}{Nd} \right)^{N-2}. \end{aligned} \tag{29}$$

Now, $f(y)$ can be defined as

$$f(y) = \lim_{N \to \infty} f_N(y) = \lambda e^{-\lambda y}, \tag{30}$$

where $\lambda = \frac{2}{d}$. The limit of $N \to \infty$ is taken by keeping $d = \frac{L}{N}$ constant. In order to perform the integral in Eq. (28), $F(v)$ was analytically calculated and numerically evaluated over its range of definition and stored in an array. One hundred million random numbers from an exponential distribution were generated as y values, and at each v, $P(v|y)$ was calculated using Eq. (27) for all y's, and it was summed over all y's. The resulting function $P(v)$ then was normalized. Figure 5 shows $P(v)$ calculated for different values of σ. The low velocity tail follows the scaling law for the low velocity tail of $F(v)$ discussed above, while the high velocity tail is independent of σ and has the exponent $\beta = -2$.

Although the behavior of the low velocity tail can be understood by the same scaling argument used in 1D system, since the low velocity tail is heavily influenced by the long distance behavior, the nearest-neighbor approximation does not hold for this region. The high velocity tail of a the two-body system, however, can be used as the nearest-neighbor approximation for the many-body system. The -2 exponent of the high velocity tail can be understood through a similar argument, but this time, by expanding $v(x)$ near its maxima, v can be written near each of its maxima as

$$v \approx v_{\max} + k_i (x - x_i)^2, \tag{31}$$

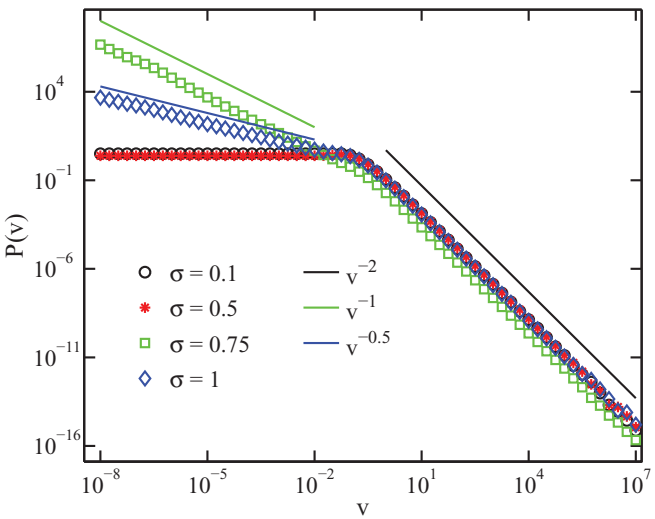

FIG. 5. (Color online) Probability distribution of velocities in ensembles of system of two particles confined in parallel lines with exponentially distributed separations, y, for $\sigma \in \{0.1, 0.5, 1.0, 1.5\}$.

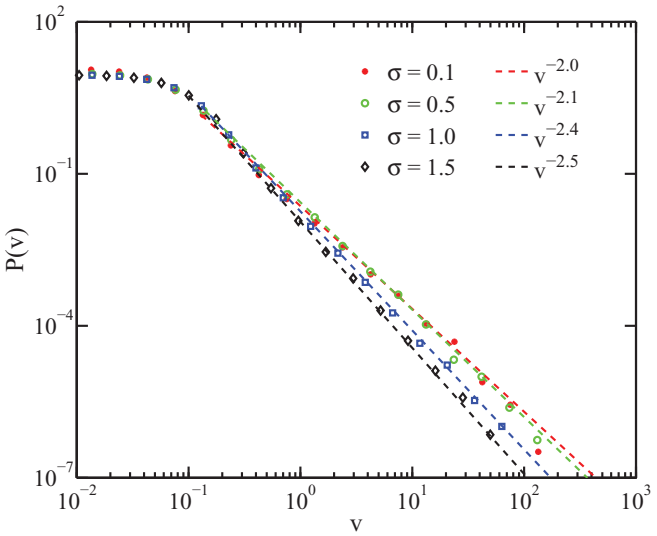

FIG. 6. (Color online) Probability distribution of velocities in a system of 200 particles ($N = 100$) for $\sigma \in \{0.1, 0.5, 1.0, 1.5\}$.

where $k_i = \frac{1}{2}\frac{\partial^2 v}{\partial x^2}|_{x_i}$ and $|v(x_i)| = v_{\max}$. Thus, using Eq. (25), near $v_{\max}$, $F(v)$ can be approximated as

$$F(v) \approx \left(\sum_i \frac{\rho(x_i)}{k_i}\right)(v_{\max} - v)^{-\frac{1}{2}}. \tag{32}$$

In other words, $F(v)$ diverges as $(v_{\max} - v)^{-\frac{1}{2}}$ in the limit that v approaches $v_{\max}$. It is important to note that the exponent does not depend on the functional form of the interaction, and this scaling holds as long as the interaction stress has a nonsingular maximum at which its second derivative does not vanish. Using Eq. (28), it is straightforward to see that the -2 exponent of the high velocity tail can be obtained only by considering the near maximum functional form $F(v)$,

$$P(v) \sim \int_0^{\frac{v_{\max}}{v}} y(v_{\max} - yv)^{-\frac{1}{2}} e^{-\lambda y} dy \sim v^{-2}. \tag{33}$$

Figure 6 shows the probability distribution for the velocity in a simulation with 200 particles ($N = 100$). The weakly temperature-dependent exponent β has the value -2 as predicted from the nearest-neighbor analysis for $\sigma \ll \sigma_c = 1$, while it has a smaller value for σ close to or larger than σ_c. This deviation from the predicted exponent in the nearest-neighbor approximation is an indication that the dislocation motion is dominated by more than just the nearest-neighbor interactions. The numerical exponent has the value $\beta = -2.4$ at the critical temperature $\sigma_c = 1$, which is consistent with the exponent found in externally driven systems at zero temperature [2].

IV. CONCLUSIONS

In this paper, we have studied the statistics of velocity fluctuations in a simplified system of dislocations with parallel Burgers vectors in 1D and 2D.

In 1D, the probability density function for the velocities of the dislocations at high velocities scales as $v^{-2-1/\sigma}$ with a power-law exponent that quantifies the strength of background noise fluctuations relative to the pairwise interaction energy. We have shown that this power-law distribution can be derived by considering only the nearest-neighbor interactions of dislocations and, therefore, is not a consequence of collective interactions.

In 2D, at an effective temperature where the noise energy $k_B T$ becomes equal to the pairwise interaction energy $\frac{\mu b^3}{2\pi(1-\nu)}$, we have found that there is a transition between a state at which the nearest neighbors are bound to each other and a state where they can escape from each other's attractive force. For temperatures significantly smaller than this transition temperature, the velocity probability density function for dislocations agrees with the scaling v^{-2} found from the nearest-neighbor analysis, while for temperatures close to or larger than this transition temperature, the probability density function follows a power-law with an exponent steeper than -2, suggesting that the high velocity events are dominated by collective effects due to the interaction of more than two dislocations. This exponent is very weakly temperature dependent and has a value of -2.4 at the transition temperature.

It remains to be further investigated how our results relate to the velocity statistics in more complicated 3D models with features such as junctions of dislocations and line tension effects.

ACKNOWLEDGMENTS

L.A. gratefully acknowledges partial support from the Center for Physics of Geological Processes at the University of Oslo.

[1] J. Weiss and J. Grasso, J. Phys. Chem. B **101**, 6113 (1997).
[2] M. Miguel, A. Vespignani, S. Zapperi, J. Weiss, and J. Grasso, Nature (London) **410**, 667 (2001).
[3] M. Uchic, D. Dimiduk, J. Florando, and W. Nix, Science **305**, 986 (2004).
[4] C. Fressengeas, A. J. Beaudoin, D. Entemeyer, T. Lebedkina, M. Lebyodkin, and V. Taupin, Phys. Rev. B **79**, 014108 (2009).
[5] D. Dimiduk, C. Woodward, R. LeSar, and M. Uchic, Science **312**, 1188 (2006).
[6] J. Weiss, T. Richeton, F. Louchet, F. Chmelik, P. Dobron, D. Entemeyer, M. Lebyodkin, T. Lebedkina, C. Fressengeas, and R. J. McDonald, Phys. Rev. B **76**, 224110 (2007).
[7] M. Zaiser, B. Marmo, and P. Moretti, Proc. Sci. (SMPRI 2005) 053.
[8] M. Zaiser, Adv. Phys. **55**, 185 (2006).
[9] M. Koslowski, R. LeSar, and R. Thomson, Phys. Rev. Lett. **93**, 125502 (2004).
[10] P. Y. Chan, G. Tsekenis, J. Dantzig, K. A. Dahmen, and N. Goldenfeld, Phys. Rev. Lett. **105**, 015502 (2010).
[11] J. Weiss and D. Marsan, Science **299**, 89 (2003).
[12] M.-C. Miguel, A. Vespignani, M. Zaiser, and S. Zapperi, Phys. Rev. Lett. **89**, 165501 (2002).
[13] G. Tsekenis, J. Uhl, N. Goldenfeld, and K. Dahmen, Europhys. Lett. **101**, 36003 (2013).

[14] J. Hirth and J. Lothe, *Theory of Dislocations* (Krieger, Malabar, 1992).
[15] M. Miguel, A. Vespignani, S. Zapperi, J. Weiss, J.-R. Grasso *et al*., Mater. Sci. Eng., A **309**, 324 (2001).
[16] M. Miguel, L. Laurson, and M. Alava, Eur. Phys. J. B. **64**, 443 (2008).
[17] P. D. Ispánovity, I. Groma, G. Györgyi, P. Szabó, and W. Hoffelner, Phys. Rev. Lett. **107**, 085506 (2011).
[18] F. F. Csikor and I. Groma, Phys. Rev. B **70**, 064106 (2004).
[19] I. Groma and B. Bakó, Phys. Rev. B **58**, 2969 (1998).
[20] P. Ispánovity, I. Groma, G. Györgyi, F. Csikor, and D. Weygand, Phys. Rev. Lett. **105**, 085503 (2010).
[21] T. Richeton, P. Dobron, F. Chmelik, J. Weiss, and F. Louchet, Mater. Sci. Eng., A **424**, 190 (2006).
[22] G. Tsekenis, N. Goldenfeld, and K. A. Dahmen, Phys. Rev. Lett. **106**, 105501 (2011).
[23] N. Friedman, A. T. Jennings, G. Tsekenis, J.-Y. Kim, M. Tao, J. T. Uhl, J. R. Greer, and K. A. Dahmen, Phys. Rev. Lett. **109**, 095507 (2012).
[24] A. J. Liu and S. R. Nagel, Nature (London) **396**, 21 (1998).
[25] P. Hähner, Appl. Phys. A **62**, 473 (1996).
[26] P. Hähner, Appl. Phys. A **63**, 45 (1996).
[27] F. Dyson, J. Math. Phys. **3**, 1191 (1962).
[28] H. Schulz, J. Phys. A **14**, 3277 (1981).
[29] C. Beenakker, Rev. Mod. Phys. **69**, 731 (1997).
[30] T. Tao, *Topics in Random Matrix Theory*, Graduate Studies in Mathematics (American Mathematical Society, Providence, Rhode Island, 2012), Vol. 132.
[31] W. König, Probab. Surv. **2**, 385 (2005).
[32] W. König, N. O'Connell, and S. Roch, Electron. J. Probab. **7** (2002).
[33] Y. V. Nazarov, Phys. Rev. Lett. **76**, 2129 (1996).
[34] P. Forrester, J. Stat. Phys. **51**, 457 (1988).